

# Nonscalar elastic light scattering from continuous random media in the Born approximation

Jeremy D. Rogers,\* İlker R. Çapoğlu, and Vadim Backman

Biomedical Engineering, Northwestern University, 2145 Sheridan Avenue, Evanston, Illinois 60208, USA

\*Corresponding author: jdrogers@northwestern.edu

Received February 19, 2009; accepted April 12, 2009;  
posted May 7, 2009 (Doc. ID 107577); published June 12, 2009

A three-parameter model based on the Whittle–Matérn correlation family is used to describe continuous random refractive-index fluctuations. The differential scattering cross section is derived from the index correlation function using nonscalar scattering formulas within the Born approximation. Parameters such as scattering coefficient, anisotropy factor, and spectral dependence are derived from the differential scattering cross section for this general class of functions. © 2009 Optical Society of America  
OCIS codes: 290.5825, 290.7050, 170.3660.

The process of elastic light scattering from weakly scattering turbid media is important in many applications ranging from radar, remote sensing, and atmospheric sciences to light propagation in biological media. Commonly used models of the continuous refractive index distributions include the Booker–Gordon formula (exponential correlation), the Gaussian model, and the Kolmogorov spectrum (von Kármán spectrum) [1]. Evidence exists for other distribution types [2], and recently several groups proposed a fractal model for index distributions of biological tissue [3,4]. In this Letter, we make use of a general model that includes the mass fractal, exponential, Gaussian, and other index correlation functions and expand on the work of Sheppard [5] to include the effect of vector waves. We also provide simplified relationships for limiting cases and discuss how the spectral dependence relates to the shape of index correlation function.

A three-parameter model with parameters  $l_c$ ,  $dn^2$ , and  $m$  is used to describe the refractive index correlation function. The model is represented by the Whittle–Matérn correlation family,

$$B_n(r) = dn^2 \frac{2^{5/2-m}}{|\Gamma(m - (3/2))|} \left(\frac{r}{l_c}\right)^{m-3/2} K_{m-3/2}\left(\frac{r}{l_c}\right), \quad (1)$$

which reduces to several important specific functions for certain values of  $m$  [6].  $K_\nu(\cdot)$  denotes the modified Bessel function of the second kind. The parameter  $l_c$  describes the index correlation distance or turbulence scale, and the parameter  $dn^2$  is the variance of the refractive index, sometimes written as  $\langle n_1^2 \rangle$ . The third parameter  $m$  determines the shape of the correlation function.

Equation (1) is normalized such that  $B_n(0) = dn^2$  for  $m > 3/2$ . As  $m \rightarrow \infty$ , the function approaches a Gaussian distribution. When  $m = 2$ , the function is a decaying exponential. Values of  $m$  between 2 and  $3/2$  result in a stretched exponential (for small values of  $r$ ). A singularity exists at  $m = 3/2$ , and the function collapses to zero because of the normalization factor of  $\Gamma(m - 3/2)$ . However, the unnormalized  $B_n(r)$  approaches a delta function for  $m = 3/2$ , and the corre-

sponding spectral density is the often used Henyey–Greenstein function. This can be interpreted as describing point like scatterers or a discrete rather than continuous medium. Values of  $m < 3/2$  correspond to a mass fractal index distribution with correlation function described by a power law, in which case  $m$  is related to the mass fractal dimension by  $d_{mf} = d_E - (3 - 2m)$ , where  $d_E$  is the Euclidean dimension. Here,  $d_E = 3$ , the dimension of the embedding medium, and is not related to the shape of the scattering bodies. Figure 1 shows  $B_n(r)$  for several representative values of  $m$ .

When  $m < 3/2$ , the function  $B_n(r)$  is infinite at  $r = 0$ , and as a consequence the function cannot be normalized. This is nonphysical, and in reality the correlation must roll off to a finite value below some minimum length scale  $r_{\min}$ . This can be represented by a truncated version of the function such that  $\tilde{B}_n(r) = B_n(r_{\min})$  for  $r < r_{\min}$ . When  $r_{\min} \ll l_c$ , the error between the model and truncated version is minimal, as discussed later. For  $r > l_c$ , the function drops quickly to zero. The model can be thought of as a fractal over the range  $r_{\min}$  to  $l_c$ , where  $r_{\min}$  is the inner length scale and  $l_c$  is the outer scale, beyond which the function drops quickly to zero.

In the Born approximation, the spectral density  $\Phi$  is the Fourier transform of  $B_n(r)$  [1]. For this model,  $B_n(r)$  is of the form of the Pearson distribution type VII,

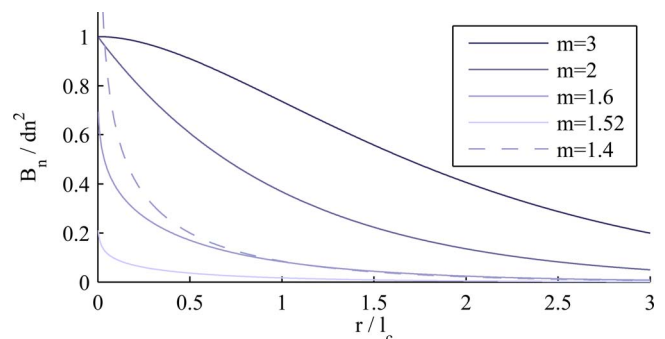


Fig. 1. (Color online) Index correlation functions for some values of  $m$ .

$$\Phi(k_s) = \mathcal{F}\{B_n(r)\} = \frac{dn^2 l_c^3 \Gamma(m)(1 + k_s^2 l_c^2)^{-m}}{\pi^{3/2} |\Gamma(m - (3/2))|}. \quad (2)$$

The spectral density is related to the differential scattering cross section per unit volume  $\sigma$  by

$$\begin{aligned} \sigma(\theta, \phi) &= 2\pi k^4 (1 - \sin^2(\theta)\cos^2(\phi))\Phi(2k \sin(\theta/2)) \\ &= \frac{2dn^2 k^4 l_c^3 \Gamma(m) (1 - \sin^2(\theta)\cos^2(\phi))}{\sqrt{\pi} |\Gamma(m - 3/2)| (1 + [2kl_c \sin(\theta/2)]^2)^m}. \end{aligned} \quad (3)$$

Note that the factor  $(1 - \sin^2(\theta)\cos^2(\phi)) = \sin^2 \chi$  depends on the polarization orientation  $\phi$  of the incident light. For  $kl_c \ll 1$  (isotropic scattering), this factor results in the dipole radiation pattern. Figure 2 (top) shows an example  $\sigma$  with slightly forward directed scattering.

The scattering coefficient  $\mu_s$  is derived by integrating  $\sigma(\theta, \phi)$  over all angles and is shown in Fig. 3. The mean-free path  $l_s$  is the inverse of the scattering coefficient  $\mu_s$ . All length scales are normalized by wavelength so that the relationships depend only on  $kl_c$  and  $kl_s$  (or  $\mu_s/k$ ),

$$\begin{aligned} \frac{\mu_s}{k} &= \frac{dn^2 \sqrt{\pi} \Gamma(m - 3)}{2k^3 l_c^3 |\Gamma(m - (3/2))|} [(1 + (2k^2 l_c^2 (m - 2) - 1) \\ &\quad \times 2k^2 l_c^2 (m - 3) - (1 + 2k^2 l_c^2 (1 + m) \\ &\quad + 4k^4 l_c^4 (4 + (m - 3)m))(1 + 4k^2 l_c^2)^{1-m})]. \end{aligned} \quad (4)$$

Equation (4) is not easy to interpret, so insight can be gained by considering the equation for either very small or very large  $kl_c$ . In the limits shown, the relationship simplifies dramatically:

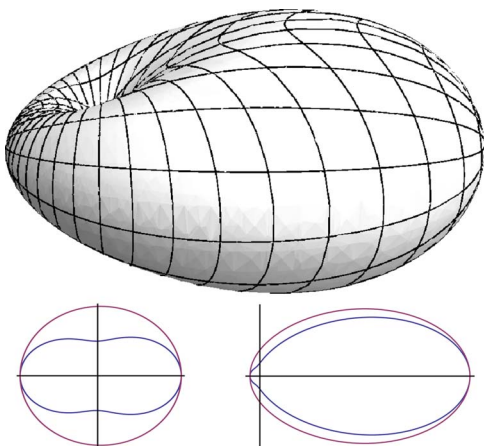


Fig. 2. (Color online) Above, example of a differential scattering cross section plotted in spherical coordinates. The incident wave propagates from left to right, and the polarization is such that electric field is in the vertical plane. The dipole is located at the origin. Below, comparison of the rotationally averaged  $\sigma_{up}$  (inner) corresponding to unpolarized incidence and the scalar wave approximation  $\sigma_{sw}$  (outer) for  $kl_c=0.1$  (isotropic scattering) shown left, and  $kl_c=1$  (forward scattering) shown right.

$$\frac{\mu_s}{k} = \begin{cases} \frac{16\sqrt{\pi}\Gamma(m)}{3|\Gamma(m - 3/2)|} dn^2 (kl_c)^3 & \text{if } kl_c \ll 1 \\ \frac{2\sqrt{\pi}\Gamma(m - 1)}{|\Gamma(m - 3/2)|} dn^2 kl_c & \text{if } kl_c \gg 1 \& m > 1 \end{cases}. \quad (5)$$

The anisotropy factor  $g$  is used to describe the degree of forward directed scattering and is defined as the average value of the cosine of the scattering angle,  $\langle \cos(\theta) \rangle$ . For this model,  $g$  is given by

$$\begin{aligned} g &= [(1 + 4k^2 l_c^2)^m (3 + 2k^2 l_c^2 (m - 4) (-3 - 4k^2 l_c^2 \\ &\quad \times (k^2 l_c^2 (m - 2) - 1)(m - 3))) - (1 + 4k^2 l_c^2) \\ &\quad \times (3 + 6k^2 l_c^2 (2 + m) + 8k^6 l_c^6 m (10 + (m - 5)m) \\ &\quad + 8k^4 l_c^4 (6 + (m - 1)m))] / [2k^2 l_c^2 (m - 4) \\ &\quad \times ((1 + 4k^2 l_c^2)^m (-1 - 2k^2 l_c^2 \times (2k^2 l_c^2 (m - 2) - 1) \\ &\quad \times (m - 3)) + (1 + 4k^2 l_c^2)(1 + 2k^2 l_c^2 (1 + m) \\ &\quad + 4k^4 l_c^4 (4 + (m - 3)m))]. \end{aligned} \quad (6)$$

Again, the limiting cases for small and large  $kl_c$  can be calculated. For  $g$  the equation in the large  $kl_c$  limit depends on the value of  $m$ ,

$$g = \begin{cases} (4/5)m(kl_c)^2 & \text{if } kl_c \ll 1 \\ 1 - \frac{1}{2(m-2)}(kl_c)^{-2} & \text{if } kl_c \gg 1 \& m > 2 \\ 1 - b2^{3-2m}(kl_c)^{2-2m} & \text{if } kl_c \gg 1 \& 1 < m < 2 \end{cases} \quad \text{where } b = \frac{(m-1)(8+m(m-5))}{(4-m)(6+m(3-m))}. \quad (7)$$

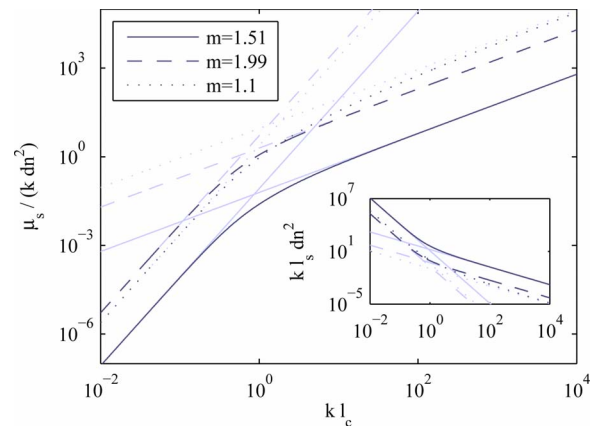


Fig. 3. (Color online) Wavelength-normalized scattering coefficient  $\mu_s/k$  as a function of wavelength normalized index correlation length  $kl_c$ . Inset, the normalized mean-free path  $kl_s = k/\mu_s$  dependence. It should be noted that although no limit is shown for  $\mu_s$ , the value is inherently limited by the requirement that  $l_s > l_c$ . This weak scattering limit requires that  $dn^2(kl_c)^2 \ll 1$ .

Combining the equations for  $\mu_s$  and  $g$  provides the reduced scattering coefficient  $\mu'_s = (1-g)\mu_s$  (or transport mean-free path,  $l'_s = 1/\mu'_s$ ). Figure 4 shows the dependence of wavelength normalized  $\mu'_s$  on  $kl_c$ .

A key feature of  $\mu'_s$  is the wavelength dependence. Measurements of  $\mu'_s$  typically exhibit a power-law dependence on wavelength [7,8]. Note that for  $kl_c \ll 1$ ,  $g \rightarrow 0$  and  $\mu'_s = \mu_s$ . In this case,  $\mu_s \propto \lambda^{-4}$ , which is consistent with Rayleigh scattering.

In most biological tissues, measurements indicate that  $g$  is large [9], implying that  $kl_c \gg 1$  [Eq. (7)]. When  $kl_c \gg 1$  and  $m > 2$ ,  $\mu'_s$  does not depend on wavelength at all. When  $kl_c \gg 1$  and  $1 < m < 2$  (the most likely regime for biological media), then  $\mu'_s \propto \lambda^{2m-4}$ . This link between the spectral dependence of the reduced scattering coefficient and the shape of the index-correlation function parameterized by  $m$  in this model enables the determination of a mass fractal dimension. Many scattering techniques can measure  $\mu'_s(\lambda)$  and thus can be used to determine  $m$  simply by determining the power-law dependence on wavelength. This spectral dependence combined with the previous relationships provides the connection between measurable optical properties  $\mu_s$ ,  $g$ ,  $\mu'_s(\lambda)$  and the model parameters  $l_c$ ,  $dn^2$ ,  $m$ .

There are two major approximations that can be made to simplify the above results. The first is needed for the mass fractal regime when  $m < 3/2$  and  $B_n(r) \rightarrow \infty$  as  $r \rightarrow 0$ . Since this situation cannot exist in reality, the actual correlation function must level off. However, this would complicate the model significantly, so provided that the error is small, the simple model can be legitimately used even for values of  $m$  that result in infinite correlation. To verify this, the normalized error is calculated numerically by computing the difference in  $\mu_s$  from the model and a truncated version of  $B_n$ , where  $\tilde{B}_n(r) = B_n(r_{\min})$  for  $r < r_{\min}$ . This approximation can be used for values of  $r_{\min} \ll l_c$ . The normalized error  $(\mu_s - \tilde{\mu}_s)/\mu_s$  is negligible for all values of  $kr_{\min}$  when  $m \rightarrow 3/2$ . As  $m \rightarrow 1$

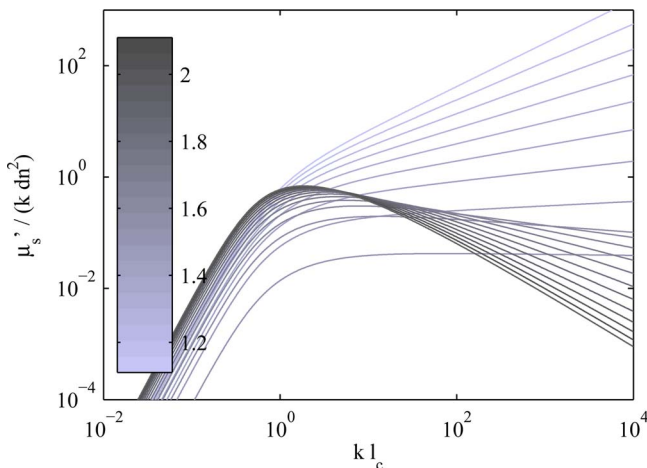


Fig. 4. (Color online) Reduced scattering coefficient as a function of index correlation length (each normalized by wavelength).

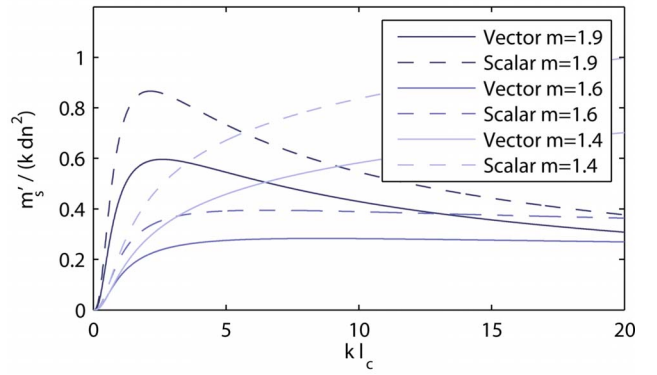


Fig. 5. Plots of  $\mu'_s$  versus  $kl_c$  with and without the dipole factor.

the error increases for large values of  $kr_{\min}$  but remains small when  $kr_{\min}$  is small. For example, for normalized error less than 1% when  $m = 1.01$  and  $kl_c = 1$ ,  $kr_{\min}$  must stay below  $1/6$ .

The second approximation that is often used is to assume scalar-wave incidence and neglect the dipole factor (dependence on  $\phi$ ), which results in an axially symmetric  $\sigma_{\text{sw}}$  (without dimples). In the case of unpolarized illumination,  $\sigma$  is sampled at all orientations of  $\phi$ , and the result can be expressed by averaging over  $\phi$  to produce a rotationally symmetric  $\sigma_{\text{up}}$ . The lower part of Fig. 2 shows the difference between the scalar-wave approximation and the result of averaging over polarization orientations. To quantify the error in this approximation, the normalized error in the scattering coefficient  $\mu_s$  is calculated and is maximum for the case of isotropic scattering where  $(\mu_s^{\text{sw}} - \mu_s)/\mu_s \rightarrow 1/2$ . The error in neglecting the dipole factor also affects the anisotropy factor  $g$  and hence  $\mu'_s$ , as shown in Fig. 5. Since this second approximation can introduce large error and the complexity of the relationships is not significantly reduced, inclusion of the dipole factor is advisable.

The authors wish to thank the National Institutes of Health (NIH) for support of this work with grants R01 EB003682 and R01 CA128641.

## References

1. A. Ishimaru, *Wave Propagation and Scattering in Random Media* (IEEE Press, 1997).
2. M. Bartek, M. Wang, W. Wells, K. Paulsen, and B. Pogue, *J. Biomed. Opt.* **11**, 064007 (2006).
3. J. M. Schmitt and J. M. Kumar, *Opt. Lett.* **21**, 1310 (1996).
4. M. Xu and R. R. Alfano, *Opt. Lett.* **30**, 3051 (2005).
5. C. J. R. Sheppard, *Opt. Lett.* **32**, 142 (2007).
6. P. Guttorp and T. Gneiting, National Research Center for Statistics and the Environment—Technical Report Series (2005).
7. J. R. Mourant, T. Fuselier, J. Boyer, T. M. Johnson, and I. J. Bigio, *Appl. Opt.* **36**, 949 (1997).
8. T. H. Pham, F. Bevilacqua, T. Spott, J. S. Dam, B. J. Tromberg, and S. Andersson-Engels, *Appl. Opt.* **39**, 6487 (2000).
9. J. F. Beek, P. Blokland, P. Posthumus, M. Aalders, J. W. Pickering, H. J. C. M. Sterenberg, and M. J. C. van Gemert, *Phys. Med. Biol.* **42**, 2255 (1997).